Exciton-exciton interaction and heterobiexcitons in GaN

S. Adachi[*] and S. Muto[†]

Department of Applied Physics, Hokkaido University, Kitaku, Sapporo 060-8628, Japan

K. Hazu, T. Sota,[‡] and K. Suzuki

Department of Electrical, Electronics, and Computer Engineering, Waseda University Shinjuku, Tokyo 169-8555, Japan

S. F. Chichibu[§]

Institute of Applied Physics; Graduate School of Pure and Applied Sciences, University of Tsukuba, 1-1-1 Tennodai, Tsukuba, Ibaraki 305-8573, Japan

T. Mukai

Nitride Semiconductor Research Laboratory, Nichia Corporation, Oka, Kaminaka, Anan, Tokushima 744-8601, Japan

The formation of not only A biexcitons (XX_{AA}) but also heterobiexcitons that consist of A and B excitons (XX_{AB}) in a free-standing bulk GaN is identified by polarization-sensitive spectrally resolved FWM measurements. The FWM spectra and delay-time dependence show that the interaction between A and B exciton gives rise to the energy shifts of the spectra and the phase shifts of the quantum beating, which is considered as the effect of the unbound state of XX_{AB} (i.e., XX_{AB}^*) and XX_{AB}^* is found to play an important role in the FWM signals for all polarizations. The unbound A biexciton (XX_{AA}^*) is also observed clearly in spectral and temporal domains.

I. INTRODUCTION

Coherent nonlinear optical processes involving bound biexcitons (XX) have been investigated extensively in bulk and quantum wells. Biexciton effects associated with XX have been identified even in III-V semiconductors and more easily in II-VI and I-VII semiconductors. However, processes involving two excitons require obviously to take account of four-particle correlations,[1–8] which mean not only XX but also unbound biexciton (XX^*). Actually, XX^* can affect the observed signals strongly even under no clear signature of XX, for example, in cocircularly polarized excitation where XX cannot be created according to the polarization selection rules. Recently, it was found that exciton-exciton correlations can have important, and even dominant, effects at low density by Kner *et al.*[8] They used the spatial confinement by magnetic field to enhance the strength of the exciton-exciton correlations. In the sense, exciton-biexciton system is an appropriate system to the investigation of many-particle correlations that are rarely accessed directly, where the scattering processes of unbound biexciton XX^* as well as XX and their correlation with the exciton scattering processes is of considerable current interest.

Gallium nitride (GaN) has large exciton binding energies of more than 20 meV because of the relatively small dielectric constant and large effective masses, and therefore, the large binding energies of biexcitons are expected. The large binding energies and strong optical nonlinearities make it suitable material for the study of biexcitons and Coulomb correlations of their excitons by using the FWM technique. Recently, the degenerate FWM has been applied to study the properties of excitons[9–12] and biexcitons[13,14] in bulk GaN. The biexcitonic contribution to the FWM signals may appear strongly in most usual excitation conditions by ultrashort pulses, and therefore is very important. But it is little known currently about the Coulomb correlations including the information of the bound biexcitons in GaN.

In this paper, we investigate experimentally the bound and unbound biexciton contributions to the spectrally resolved FWM signals in a free-standing bulk GaN. The spectra of heterobiexciton XX_{AB} that consists of A- and B-hole excitons as well as A-hole bound (XX_{AA}) and unbound (XX_{AA}^*) biexcitons were clearly observed. Observation of XX_{AB} in GaN is for the first time to our best knowledge. The unbound XX_{AB}^* is essential for the X_A-X_B interaction and contributes more significantly to the FWM signal generation rather than the bound XX_{AB} biexcitons.

II. SAMPLE AND EXPERIMENT

The investigated sample is a free-standing *c*-face wurtzite GaN of 70-μm thickness by the two-flow metal-organic chemical vapor deposition method[15] using the lateral epitaxial overgrowth technique.[16,17] GaN crystallizes in the wurtzite structure, whose valence bands consist of A, B, and C bands that are split each other even at Γ point due to the crystal field and spin-orbit interaction.[18] Therefore, the corresponding exciton structure consists of A, B, and C excitons (denoted hereafter as X_A, X_B, and X_C, respectively). The transition energy difference between X_A and X_B is known to be 5-6 meV, and the X_C resonance is apart by more than 10 meV from the X_B resonance.

The spectrally resolved, time-integrated two-pulse FWM experiments in reflection geometry are performed with the excitation pulses of the same intensities in the directions $\boldsymbol{k}_1$ and $\boldsymbol{k}_2$, respectively. The pulses from a frequency-doubled,

67 205212-1

mode-locked Ti-doped sapphire laser with the spectral width of 17.5 meV (FWHM) is used as a light source. The emitted FWM signal in the $2\boldsymbol{k}_2-\boldsymbol{k}_1$ direction is spatially selected by an iris, spectrally resolved by a spectrometer with the resolution of 0.9 meV (FWHM), and detected phase sensitively by a photomultiplier. The delay time τ_{12} between the two incident pulses is defined to be positive if the $\boldsymbol{k}_1$ pulse precedes the $\boldsymbol{k}_2$ pulse. The total excitation intensity is 140 nJ/cm^2, corresponding to the excited exciton densities of $\sim 10^{16}$ cm^{-3}, which is two orders of magnitude smaller than the screening density ($\sim 2\times 10^{18}$ cm^{-3}). The sample is placed in a closed-cycle helium cryostat and all presented FWM data are taken at 10 K. The detail of the experimental setup is seen in Ref. 12.

III. RESULTS AND DISCUSSIONS

Polarization selection rules in FWM can be used to discriminate transitions from the vacuum state (G) to one of the optically active exciton states (X) or transitions from X to bound biexciton states (XX) (see Fig. 2). The FWM signal originates from the nonlinearities of phase-space filling (PSF), bare Coulomb interaction (BCI), and exciton-exciton correlation (XXC), which is significantly dependent of light polarizations and temporal ordering of the excitation pulses via the parametric relation between coherently created polarizations and occupations of the involved transitions and states. Here BCI means Coulomb nonlinearities within the Hartree-Fock treatment and the interaction to induce band-edge renormalization and local-field effect.[19]

Figure 1(a) shows the FWM spectra at $\tau_{12}=0.8$ ps and for different polarization configurations. The labels X_B, X_A, and XX_{AA} represent the B-exciton, A-exciton, and the bound A-biexciton states, respectively. The arrows on the top axis point to the energies of the transverse X_A (3.4791 eV) and X_B (3.4844 eV) resonances that were obtained from the analysis of the reflection spectra.[20] Thus, X_A-XX_{AA} corresponds to the transition energy from X_A to XX_{AA}. From the position of X_A-XX_{AA}, the XX_{AA}-binding energy is found to be 5.3 meV. We have tuned the center laser wavelength energetically below the X_A resonance as shown in Fig. 1(a), in order to minimize the excitation of X_C and exciton continua. X_C resonance locates by 18.3 meV above X_B resonance in this sample. The transition matrix element μ_A of X_A is larger by a small amount than μ_B of X_B (the calculated ratio $\mu_A^2:\mu_B^2\sim 1:0.88$) and the FWM signals are proportional to $N_i^2\mu_i^8$ ($i=A$, B), where N_i is the density of the corresponding exciton state. Consequently, the FWM signal at X_A are stronger than that at X_B.

The relative contributions between X_A and XX_{AA} to the FWM signal are dependent strongly of the excitation polarization. For cocircular polarizations (σ_+,σ_+), the transition from X_A (X_B) to XX_{AA} (XX_{BB}) is not allowed since XX_{AA} (XX_{BB}) consists of two X_As (X_Bs) with opposite exciton spin and has the angular momentum $J_z=0$. Thus, the signal X_A-XX_{AA} does not appear in (σ_+,σ_+) spectra. The X_A line broadens with relatively small inhomogeneity compared with the temporal FWM trace (Fig. 3) that decays with the time constant of 0.66 ps for $\tau_{12}>0$. The decay constant
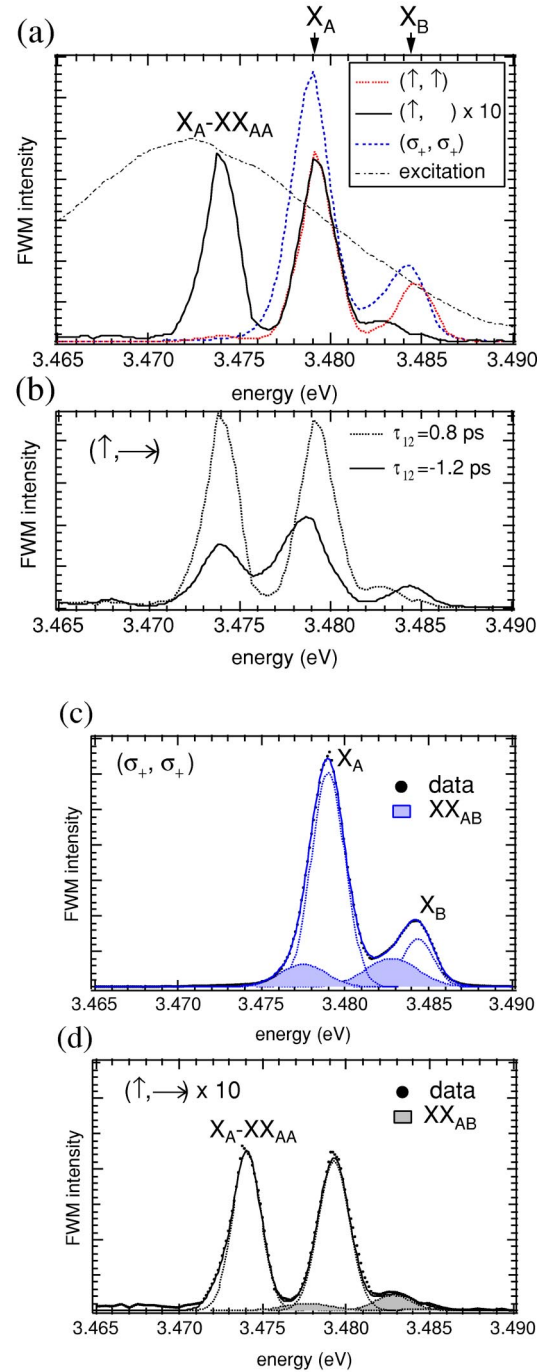

FIG. 1. (a) FWM spectra at $\tau_{12}=0.8$ ps. The three excitation polarizations are used as indicated. The spectrum in ($\uparrow,\rightarrow$) polarizations is multiplied by 10. The arrows at the top axis indicate the energies of A- and B-exciton resonances obtained by the reflection spectra. The excitation spectrum is also indicated. (b) FWM spectra in ($\uparrow,\rightarrow$) at positive [$\tau_{12}=0.8$ ps, same as (a)] and negative ($\tau_{12}=-1.2$ ps) delay times. (c) and (d) The fitting results of FWM spectra at $\tau_{12}=0.8$ ps. The solid circles and dotted lines are the experimental data and the decomposed peaks. The solid line is the total fitted spectrum. The shaded components indicate the hetero-biexcitons XX_{AB} that consist of X_A and X_B. Note that these components are seen at the lower-energy side of X_A and X_B in all polarization configurations shown in Fig. 1(a).
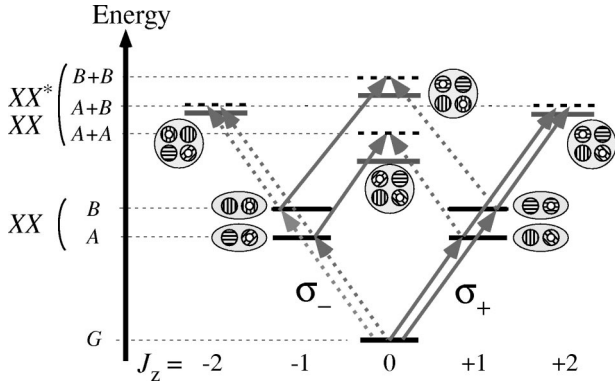
FIG. 2. Level diagram of exciton-biexciton system for a helicity basis. The thick solid lines represent exciton X and *bound* biexciton XX states to which the transitions are allowed. The thick dashed lines above the bound biexciton states indicate the corresponding biexciton continuum edge ($2X$). X's and XX's are illustrated with their constituent electrons and holes. Electron is depicted as a circle with vertical ($m_J^c = -1/2$) or horizontal lines ($m_J^c = 1/2$). Hole is as a double circle with vertical ($m_J^v = 1/2$), horizontal ($m_J^v = -1/2$), right-oblique ($m_J^c = 3/2$), and left-oblique ($m_J^c = -3/2$) lines.

corresponds to the homogeneous broadening of 500 μeV and therefore the ratio $\Gamma_{inhomo}/\Gamma_{homo}$ is found to be ~ 4. Taking account into the exciton lifetime and acoustic phonon scattering of this sample,[12] the broadening consists of 330 μeV by radiative broadening, 90 μeV by acoustic phonon scattering, and ~ 80 μeV by density-dependent broadening under these experimental conditions.

For cross-linear polarization ($\uparrow, \rightarrow$), the signals at the energies of X_A and X_B are strongly suppressed by the quenching of the signal generation due to excitation-induced dephasing (EID),[21,22] which is a part of XXC, and the signal intensity at the energy of X_A becomes comparable to the X_A-XX_{AA} signal. Note that, in Fig. 1(a), the ($\uparrow, \rightarrow$) signal is
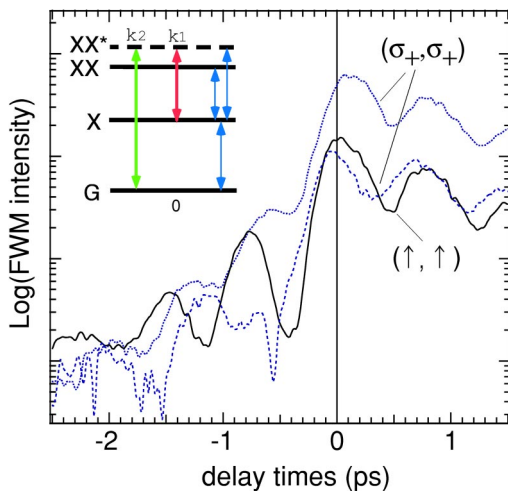

FIG. 3. Spectrally resolved FWM traces at X_A energy as a function of τ_{12} for (σ_+, σ_+) at G-X_A (dotted line), at G-X_B (dashed line), and ($\uparrow, \uparrow$) at G-X_A (solid line). Inset, a simple level diagram for the signal generation process. Note that both X_A and X_B are excited in the experiment.

multiplied by 10. From the polarization selection rules, the FWM signal in the direction $2\mathbf{k}_2$-$\mathbf{k}_1$ for $\tau_{12} > 0$ should arise from the X_A-XX_{AA} and X_A-XX_{AA}^* transitions for ($\uparrow, \rightarrow$). Thus, the observed FWM signal in the vicinity of the energy of X_A is associated with the unbound biexciton XX_{AA}^*. From the fact that the transition energies G-X_A and X_A-XX_{AA}^* are the same within our spectral resolution and X_A-XX_{AA} and X_A-XX_{AA}^* transitions have the comparable strength and width that is the same as G-X_A for (σ_+, σ_+), the following are found; the unbound state XX_{AA}^* locates at the edge of two A-exciton continuum, the X_A-XX_{AA}^* transition has the similar magnitude of the matrix element as X_A-XX_{AA}, and the broadenings of X_A, XX_{AA}, and XX_{AA}^* have a nearly perfect correlation. This is quite reasonable for this bulk sample with small inhomogeneity. Recently, Langbein *et al.*, observed that the XX_{AA}^* state moves from the $2X_A$-continuum edge to higher energetic region, increasing inhomogeneity due to the well-width fluctuation in GaAs quantum wells.[23] As compared with Fig. 1(b), the contribution in the vicinity of X_A-XX_{AA}^* and X_B-XX_{BB}^* changes significantly, whereas the central energy of the X_A-XX_{AA} spectrum does not change when the delay time τ_{12} varies from negative to positive values. The effect can be explained by XX_{AB} that will be discussed later.

For colinear polarization ($\uparrow, \uparrow$), the X_A-XX_{AA} component can appear also in accordance with the polarization selection rules, and in fact, the small peak was observed in the spectra though the component is much smaller compared with the signal at G-X_A transition. Same as the case for ($\uparrow, \rightarrow$), X_A-XX_{AA}^* may contribute to similar extent at the energy of X_A. In addition, two main peaks at X_A and X_B are found to be blue shifted slightly from the (σ_+, σ_+) spectra and is not shifted from the ($\uparrow, \rightarrow$) spectra. The blue shift can be explained by the spin-dependent X_A-X_B interaction (i.e., XX_{AB}^*) and therefore is seen also in ($\uparrow, \rightarrow$) spectra. Here, the X_A-X_B interaction means the correlation via PSF in electronic spin states of X_A and X_B. For example, as shown in Fig. 2, the states X_A and X_B with $J_z = 1$ can be represented as $|3/2, -3/2, 1/2, -1/2\rangle$ and $|1/2, -1/2, 1/2, 1/2\rangle$ in $|J^v, m_J^v, J^c, m_J^c\rangle$.

While these X_A and X_B with the same exciton spins that are created in a broadband (σ_+, σ_+) excitation, have different electronic spin states and no PSF occurs in any state, PSF occurs in the electron spins in ($\uparrow, \uparrow$) and ($\uparrow, \rightarrow$) excitations because X_A and X_B with different exciton spins are created simultaneously. Thus, *with opposite exciton spins*, the attractive force works between the same species (X_A-X_A and X_B-X_B) and makes the bound biexciton X_{AA} and X_{BB}, and the repulsive force works between the different species (X_A-X_B). Conversely, *with the same exciton spins*, the attractive force works between X_A and X_B and the repulsive force works between the same species. This X_A-X_B interaction can be considered as the effect of XX_{AB}^*. This effect gives rise also to the phase shift of X_A-X_B quantum beats in the temporal evolution as seen in Fig. 3. The influence of X_A-X_B interaction on the phase shift of X_A-X_B quantum beats was analyzed by Aoki *et al.* by using weakly interacting Boson model.[11]

Figures 1(c) and 1(d) show the examples of the decomposition of the FWM spectra. The fitting was performed assuming that Gaussian line shape in accordance with the inhomogeneous broadening. As a result, for all polarization configurations, $(\uparrow, \uparrow)$, $(\uparrow, \rightarrow)$, and (σ_+, σ_+), two weak and relatively broad components appear at the energies by ~ 1.4 meV in the low-energy side of X_A and X_B. The components are indicated by the shade in the figures. Without these components, for example, the trough between X_A and X_B for (σ_+, σ_+) or the small peak at the wing of X_B is not possible to be sufficiently reproduced. Those components also appeared in the FWM spectra at negative τ_{12} and for all polarization configurations.

The fact, those components are observed at the lower-energy side apart by the same amount from both X_A and X_B resonances regardless of the polarization configurations and the sign of the delay times, leads to the presence of the heterobiexciton XX_{AB} that consists of X_A and X_B as a bound biexciton state. The heterobiexciton has been observed also in a 100-Å-ZnSe single-quantum well by FWM (Ref. 24) and a bulk ZnO by two-photon reabsorption spectroscopy.[25] The bound biexcitons that consist of the same species, XX_{AA} and XX_{BB}, have paired electron spins as well as hole spins, and $J_z = 0$. On the other hand, XX_{AB} has different hole spins and opposite electron spins, and therefore their J_z are ± 2 as shown in Fig. 2. Reflecting the low density of X_B compared with X_A, the XX_{AB} component in the lower wing of X_B is larger than that in the lower wing of X_A. From the observed spectra, the binding energy of XX_{AB} is 1.4 meV that corresponds to the period of ~ 3 ps if quantum beats between X_α-XX_{AB} and X_α-XX_{AB}^* ($\alpha = A$, B) occurs. Unfortunately, small population of XX_{AB} as well as the long period compared with the phase relaxation time smear the beating in temporal domain. In general, the biexciton binding energy has the tendency that the binding energy is increasing with decreasing electron-hole mass ratio m_e^*/m_h^*, and the measured value is on this tendency.

The precise interpretation of XXC requires the formalisms to handle n-particle correlations such as dynamics controlled truncation scheme (DCTS),[26] where the coupled equations of motion of one-pair and two-pair correlations at least have to be computed. Since it is difficult to carry out for our experimental situation as shown in Fig. 2, instead we will survey the temporal behavior qualitatively in the light of the XXC, particularly, the X_A-X_B interaction which is nothing but XX_{AB}^*.

Figure 3 shows the spectrally resolved FWM traces as a function of τ_{12} at the energy of X_A. For the comparison, the signals for (σ_+, σ_+) at X_B energy (dashed line) is also depicted. The signal decay for $\tau_{12} > 0$ is well fitted with the time constant of 0.66 ps by using a suitable equation for intermediate inhomogeneous broadening and the decay time is nearly the same for all polarization configurations. Fundamentally, the signal for $\tau_{12} > 0$ shows the decay of the first-order polarization created by k_1 pulse that drives the G-X_A transition. The signal intensities in (σ_+, σ_+) and $(\uparrow, \uparrow)$ are approximately one order of magnitude stronger than that in $(\uparrow, \rightarrow)$ (not shown here) at $\tau_{12} > 0$, which shows that the

EID-induced process is strongly suppressed for $(\uparrow, \rightarrow)$. Thus, XXC (XX_{AA}^* and XX_{AB}^* in this case) contributes strongly to the FWM signal even at $\tau_{12} > 0$. This signal intensity ordering observed as well as in the FWM spectra has been measured generally in GaAs-based materials, which is determined by the magnitudes of XX_{AA}^*, XX_{AB}^* and the phase between them. All the FWM signals indicate the clear beating character. The beating for (σ_+, σ_+) and $(\uparrow, \uparrow)$ signals is well reproduced with the frequency of 1.31 THz, corresponding to 5.4 meV. The energy coincides well to the energy difference between X_A and X_B (5.3 meV) from linear spectroscopies. From the beat period and π-phase-shift character for $(\uparrow, \rightarrow)$ against (σ_+, σ_+) and $(\uparrow, \uparrow)$ signals, the beating can be assigned to X_A-X_B quantum beat. The initial phase of the quantum beat in (σ_+, σ_+) is shifted by 0.4π compared with the beat in $(\uparrow, \uparrow)$. For X_B (not shown in Fig. 3), the phase shift has an opposite sign ($\sim -0.15\pi$). This spin-dependent X_A-X_B interaction induces the phase shift as well as the aforementioned energy shift in the FWM spectra [Fig. 1(a)].

For $\tau_{12} < 0$, the signal should be entirely due to the Coulomb-induced nonlinearities. It is expected that the bound biexcitons, such as XX_{AA}, XX_{BB}, and XX_{AB}, will make a more noticeable contribution in processes where two-photon transitions are active, i.e., for negative delay times, and their continua or their unbound biexcitons play a minor role. But this is not the case. In ideal case, because the pulse with the wave vector k_2 arrives first at the sample for $\tau_{12} < 0$ and the contribution to signal generation process is in second order as shown in the inset of the figure, the signal generation due to PSF is suppressed for all polarizations. Instead, two-photon coherences (TPC's) created[2] by two k_2 photons dominate the dynamics of the system. Since the two-exciton state as a source of XXC is created by this two-photon transition, it cannot emit light and builds up until the k_1 pulse arrives and triggers the FWM emission. The slow rise of the signals that are very similar to the rise time of X_A-XX_{AA}, therefore, suggests that the signals are related to the TPC's. Especially, for (σ_+, σ_+) polarizations where the creation of XX_{AA} is inhibited, the slow rise is unexpected without XXC since the signal should rise with a shorter time constant than half the decay time for $\tau_{12} > 0$ at least in the case that any XXC's do not work. XX_{AA}^* and XX_{AB}^* contribute to the signal and the clear beating indicates the existence of XX_{AB}^*. For (σ_+, σ_+), the beating period for $\tau_{12} < 0$ is almost the same as that for $\tau_{12} > 0$ and there is no phase jump around $\tau_{12} = 0$. Under no signal generation pathway via PSF, this means that the beating originates from XX_{AB}^*-TPC-induced interference between the transitions X_A-XX_{AB}^* and X_B-XX_{AB}^*. A pronounced beating for $(\uparrow, \uparrow)$ has a higher contrast than that for $\tau_{12} > 0$ and indicates the significant XX-TPC and XX^*-TPC contributions. The beating originates from the interference between the signals induced by the TPC's and the XXC is attributed mainly to the correlation between XX_{AA}^* and XX_{AB}^*. For the quantitative explanation, the computational challenge for this system are currently proceeded.

IV. SUMMARY

In summary, we have investigated the FWM responses of the exciton-biexciton system in a free-standing GaN. The spectrally resolved FWM signals were discussed in terms of biexciton formation and its contribution were explained qualitatively. The formation of not only A biexcitons XX_{AA} ($\Delta E_b^{AA} = 5.3$ meV) but also a heterobiexciton XX_{AB} ($\Delta E_b^{AB} = 1.4$ meV) has been identified by polarization selection rules. The unbound XX_{AB}^* is essential for the X_A-X_B interaction and contributes more significantly to the FWM signal generation rather than the bound XX_{AB} biexcitons, especially, for (σ_+, σ_+) and $(\uparrow, \rightarrow)$ polarizations.

*Electronic address: adachi-s@eng.hokudai.ac.jp

†CREST, Japan Science and Technology Corporation, Kitaku, Sapporo 060-8628, Japan.

‡Also at Integrative Bioscience and Biomedical Engineering, Graduate School of Science and Engineering, Waseda University, Shinjuku, Tokyo 169-8555, Japan.

§NICP, ERATO, Japan Science and Technology Corporation, 2-4-6 Fujimi, Chiyoda-ku, Tokyo 102-0071, Japan and Photodynamics Research Center, RIKEN, Aoba, Sendai, Miyagi 980-0845, Japan.

[1] A.L. Ivanov, H. Wang, J. Shah, T.C. Damen, L.V. Keldysh, H. Haug, and L.N. Pfeiffer, Phys. Rev. B **56**, 3941 (1997).

[2] K.B. Ferrio and D.G. Steel, Phys. Rev. B **54**, R5231 (1996).

[3] E.J. Mayer, G.O. Smith, V. Heuckeroth, J. Kuhl, K. Bott, A. Schulze, T. Meier, S.W. Koch, P. Thomas, R. Hey, and K. Ploog, Phys. Rev. B **51**, 10 909 (1995).

[4] K. Bott, O. Heller, D. Bennhardt, S.T. Cundiff, P. Thomas, E.J. Mayer, G.O. Smith, R. Eccleston, J. Kuhl, and K. Ploog, Phys. Rev. B **48**, 17 418 (1993).

[5] A.E. Paul, J.A. Bolger, A.L. Smirl, and J.G. Pellegrino, J. Opt. Soc. Am. B **13**, 1016 (1996).

[6] H.P. Wagner, A. Schätz, W. Langbein, J.M. Hvam, and A.L. Smirl, Phys. Rev. B **60**, 4454 (1999).

[7] W. Langbein, T. Meier, S.W. Koch, and J.M. Hvam, J. Opt. Soc. Am. B **18**, 1318 (2001).

[8] P. Kner, W. Schäfer, R. Lövenich, and D.S. Chemla, Phys. Rev. Lett. **81**, 5386 (1998).

[9] A.J. Fischer, W. Shan, G.H. Park, J.J. Song, D.S. Kim, D.S. Yee, R. Horning, and B. Goldenberg, Phys. Rev. B **56**, 1077 (1997).

[10] S. Pau, J. Kuhl, F. Scholz, V. Haerle, M.A. Khan, and C.J. Sun, Phys. Rev. B **56**, R12718 (1997).

[11] T. Aoki, G. Mohs, M. Kuwata-Gonokami, and A.A. Yamaguchi, Phys. Rev. Lett. **82**, 3108 (1999).

[12] K. Hazu, A. Shikanai, T. Sota, K. Suzuki, S. Adachi, S.F. Chichibu, and T. Mukai, Phys. Rev. B **65**, 195202 (2002).

[13] R. Zimmermann, A. Euteneuer, J. Möbius, D. Weber, M.R. Hofmann, W.W. Rühle, E.O. Göbel, B.K. Meyer, H. Amano, and I. Akasaki, Phys. Rev. B **56**, R12722 (1997).

[14] K. Kyhm, R.A. Taylor, J.F. Ryan, T. Aoki, M. Kuwata-Gonokami, B. Beaumont, and P. Gibart, Phys. Status Solidi B **228**, 475 (2001).

[15] For a review, S. Nakamura and G. Fasol, *The Blue Laser Diode* (Springer-Verlag, Heidebelg, 1997).

[16] A. Usui, H. Sunakawa, S. Sakai, and A.A. Yamaguchi, Jpn. J. Appl. Phys. **36**, L899 (1997).

[17] S. Nakamura, M. Senoh, S. Nagahama, N. Iwasa, T. Yamada, T. Matsushita, H. Kiyoku, Y. Sugimoto, T. Kozaki, H. Umemoto, M. Sano, and K. Chocho, Jpn. J. Appl. Phys. **37**, L309 (1998).

[18] M. Suzuki, T. Uenoyama, and A. Yanase, Phys. Rev. B **52**, 8132 (1995).

[19] J. Shah, *Ultrafast Spectroscopy of Semiconductors and Semiconductor Nanostructures* (Springer-Verlag, New York, 1998).

[20] K. Torii, T. Deguchi, T. Sota, K. Suzuki, S. Chichibu, and S. Nakamura, Phys. Rev. B **60**, 4723 (1999).

[21] H. Wang, K. Ferio, D.G. Steel, Y.Z. Hu, R. Binder, and S.W. Koch, Phys. Rev. Lett. **71**, 1261 (1993).

[22] Y.Z. Hu, R. Binder, S.W. Koch, S.T. Cundiff, H. Wang, and D.G. Steel, Phys. Rev. B **49**, 14 382 (1994).

[23] W. Langbein and J.M. Hvam, Phys. Status Solidi A **190**, 167 (2002).

[24] H.P. Wagner, W. Langbein, and J.M. Hvam, Phys. Rev. B **59**, 4584 (1999).

[25] J.M. Hvam, G. Blattner, M. Reuscher, and C. Klingshirn, Phys. Status Solidi B **118**, 179 (1983).

[26] V.M. Axt and A. Stahl, Z. Phys. B: Condens. Matter **93**, 195 (1994).